

# Tensile properties of a nanocrystalline 316L austenitic stainless steel

X.H. Chen <sup>a</sup>, J. Lu <sup>b</sup>, L. Lu <sup>a</sup>, K. Lu <sup>a,\*</sup>

<sup>a</sup> Shenyang National Laboratory for Materials Science, Institute of Metal Research, Chinese Academy of Sciences, 72 Wenhua Road, Shenyang 110016, PR China

<sup>b</sup> LASMIS, FRE CNRS 2719, University of Technology of Troyes, 10000 Troyes, France

Received 27 September 2004; received in revised form 26 December 2004; accepted 17 January 2005

## Abstract

A nanocrystalline 316L austenitic stainless steel sample (mean grain size  $\sim 40$  nm) was prepared by means of surface mechanical attrition treatment. Uniaxial tensile tests at room temperature showed the nanocrystalline sample exhibits an extremely high yield strength up to 1450 MPa, which still follows the Hall–Petch relation extrapolated from the coarse-grained material.

© 2005 Acta Materialia Inc. Published by Elsevier Ltd. All rights reserved.

**Keywords:** Nanocrystalline materials; Surface mechanical attrition treatment; Tensile properties; 316L austenitic stainless steel

## 1. Introduction

316L austenitic stainless steel is nowadays a widely used engineering material due to its excellent corrosion and oxidation resistance and good formability. However, application of this material is hindered by its low mechanical strength and poor anti-friction properties. Strengthening the stainless steel has drawn much attention in the past decades and various approaches have been developed, such as varying its chemical compositions to induce solid solution hardening [1,2] and grain refinement [3–5].

On refining grains of 316L stainless steel, several techniques have been used in which coarse grains are refined via plastic deformation and/or subsequent recrystallization, including mechanical milling (MM) [3], cold rolling (CR) [4], and severe plastic deformation (SPD) [5]. 316L powders were mechanically milled and sintered at 1173 K for 3.6 ks, forming a bulk sample with an ultrafine-grained structure (average grain size  $\sim 250$  nm) [3].

Its hardness is up to 6.2 GPa, which is about 4.4 times that of coarse-grained (CG) 316L. An ultrafine-grained 316L sample was produced by means of heavy cold working at 77 K followed by annealing at 973 K, of which the yield strength ( $\sigma_y$ ) is as high as 1280 MPa [4]. Pakiela et al. [5] prepared a nanostructured 316L with grain size of 65 nm using high pressure torsion, reaching a tensile strength of about 1340 MPa. However, during these processes a martensite transformation occurred as well as the grain refinement. Presence of a considerable amount of martensite in the processed samples is harmful to anti-corrosion properties of this material [6]. Thereby, it is of significance to develop a processing technique that can not only effectively refine austenitic grains but also keep the austenitic structure of 316L.

Surface mechanical attrition treatment (SMAT) is a recently developed technique that can effectively induce grain refinement into nanometer regime in surface layer (of several tens of micrometers thick) of bulk materials [7–10]. The nanocrystalline (nc) layer is free of contamination and porosity because the nanocrystallization process is induced by severe plastic deformation at very high strain rates [8]. The grain size of the processed

\* Corresponding author. Tel.: +86 24 23906826; fax: +86 24 2399 8660.

E-mail address: [lu@imr.ac.cn](mailto:lu@imr.ac.cn) (K. Lu).

surface layer can be as small as 10 nm in some materials. Previous preliminary investigations [11] showed that no martensite phase transformation occurred in 316L during the SMAT processing. In this work, we produced a nc 316L on the surface of a CG plate by means of the SMAT technique. Mechanical properties of the nc 316L samples free of contamination and porosity were investigated with respect to its microstructural characteristics.

## 2. Experimental procedures

Nanocrystalline 316L samples were prepared by using the SMAT technique. The material used for SMAT processing was a 316L sheet (1 mm thick) with a chemical composition of 0.019 C, 17.07 Cr, 11.95 Ni, 2.04 Mo, 1.68 Mn, 0.35 Si, 0.04 Cu and 0.007 S (mass%). The initial material was a face-centered cubic (fcc) austenite with grain sizes ranging between 5 and 50  $\mu\text{m}$ , averaging 20  $\mu\text{m}$ .

The setup of SMAT processing can be found in previous publications [7,8,10]. The basic principle of treatment is the generation of plastic deformation in the top surface layer of a bulk material by means of a large number of repeated multidirectional impacts of flying balls onto the sample surface over a short period of time. The induced plastic deformation in the surface layer with a large strain and a high strain rate results in a progressive refinement of coarse grains into the nanometer regime.

The main parameters of SMAT processing used in present work are as follows: the vibration frequency of the chamber driven by an ultrasonic generator of 4 kW was 20 kHz, the ball (stainless steel) diameter was 3 mm, and the duration of the treatment was 30 min. A nc layer of 316L of about 20  $\mu\text{m}$  thick was formed after SMAT. Underneath the nc layer, the grain sizes increase gradually from the nanometer to the micrometer scale.

Nanocrystalline 316L samples for tensile tests were prepared as follows. Firstly, the top surface layer of about 3  $\mu\text{m}$  thick in the SMAT sample was removed by mechanical polishing to eliminate the surface roughness effect on tensile properties. Dogbone-shaped tensile specimens were cut from the top surface layer (about 20  $\mu\text{m}$  thick) by using electro-discharging followed by mechanical polishing. Finally, the samples were electro-polished to a mirror finish with a final thickness of about 15  $\mu\text{m}$ . The final tensile sample geometry has a gauge length of 4 mm, a cross-sectional area of 2 mm  $\times$  0.015 mm and the radius between the gauge length and the grip ends of 2.5 mm, as shown in insert of Fig. 2. To ensure the small scatter of the tensile data, accurate measurements of the dimensions (gauge size

and thickness) of the tensile specimens were performed carefully by means of SEM observations. Four repeated tensile tests were performed on the tested samples.

Tensile tests were performed on a Tytron 250 Microforce Testing System (produced by MTS System Corporation, with a precision of force measurement of 10 mN) at a strain rate  $6 \times 10^{-3} \text{ s}^{-1}$  at room temperature. A contactless MTS LX300 Laser extensometer was used to calibrate and measure the strain of the tested sample during loading. For comparison, a CG 316L sample (original, before the SMAT) was also tested at the same conditions. Parallel hardness measurements were also performed with a MVK-H300 Vickers hardness testing machine, with a load of 5 g and a loading time of 10 s.

The microstructure of 316L samples was characterized by using a Rigaku D/max 2400 X-ray diffractometer (12 kW) and a Philips EM420 transmission electron microscopy (TEM) operated at a voltage of 120 kV. Thin foil samples for TEM observations were ion-thinned at low temperatures. Fracture surfaces after tensile test of sample were examined on a Cambridge JSM-6301F scanning electron microscopy (SEM).

## 3. Results and discussion

The XRD pattern of nc 316L sample shows a fcc austenite phase without any evidence of martensite. The diffraction lines of austenite phase are obviously broadened in comparison with those of original CG sample. The average grain size of top layer with a thickness of 6  $\mu\text{m}$  of the nc 316L sample is about 22 nm, as estimated from the XRD line broadening. Grain sizes increase gradually with an increasing depth from the top surface. No texture is identified from the XRD pattern in the treated nc sample.

Fig. 1 shows bright field and dark field TEM images of nc 316L sample at center of the tensile specimen (about 6–8  $\mu\text{m}$  deep from the polished top surface). Observations show nc grains are mostly equiaxed with random crystallographic orientations as indicated in selected area electron diffraction (SAED) patterns (Fig. 1(c)). Grain sizes measured from a number of bright and dark field images indicate a narrow size distribution with an average value of about 40 nm (as shown in Fig. 1(d)). The difference in average grain sizes derived from TEM and XRD analyses may originate from the fact that XRD averages information over a thicker sample (about 6  $\mu\text{m}$ ) than that in the TEM sample (less than 0.5  $\mu\text{m}$ ).

Uniaxial tensile true stress–strain curves of the nc and the CG 316L samples are shown in Fig. 2. Obviously, the nc sample exhibits a much higher strength compared with its CG counterpart. The yield strength (0.2% offset) reaches as high as  $1450 \pm 60 \text{ MPa}$ , about 6 times that of

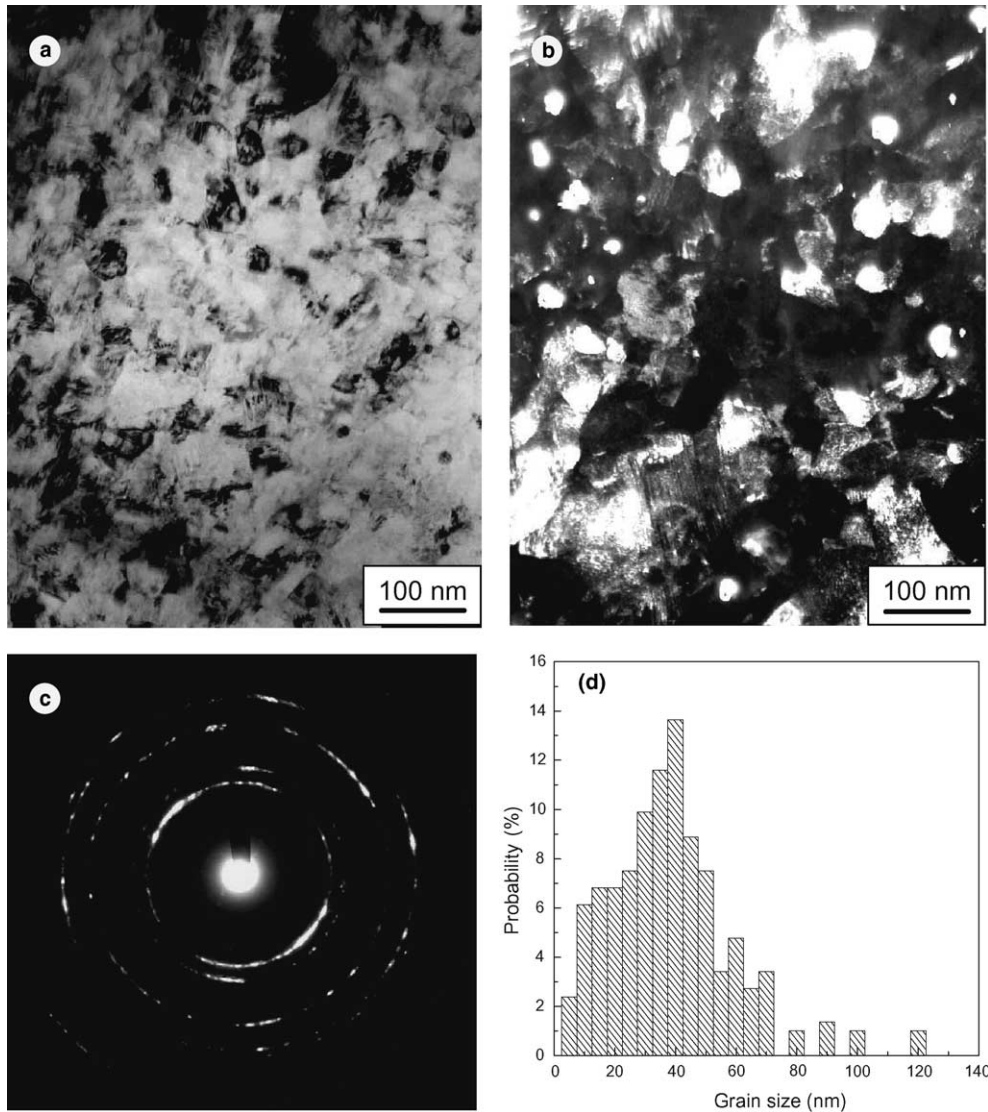


Fig. 1. Planar-view bright field TEM image (a), dark field TEM image (b) and a corresponding SAED pattern (c) showing the microstructures at 11  $\mu\text{m}$  underneath the surface of the 316L sample after SMAT processing. (d) Grain size distribution determined from TEM observations.

CG sample (250 MPa), and the ultimate tensile strength is  $1550 \pm 80$  MPa. The Vickers hardness of the nc sample is 4.5 GPa. Good agreement of the measured  $\sigma_y$  and Vickers hardness (divided by 3) implies nc 316L sample is fully dense and free of porosity.

The plasticity is depressed for the nc sample, with an elongation-to-failure of about 3.4%. Some strain hardening is observed during the plastic deformation prior to fracture. The strain hardening exponent ( $n$ ) for samples can be derived by fitting the equation  $\sigma = K\epsilon^n$  to the uniform plastic deformation section of the true stress-strain curve well beyond the yield point. The  $n$  value for the nc sample ( $n = 0.072$ ) is found to be much smaller than that for the CG ( $n = 0.385$ ). Nc grains tend to lose work hardening significantly on deformation owing to their very low dislocation storage efficiency inside tiny

grains. At the same time, this weak strain hardening also indicates that some lattice dislocation accumulation happened during plastic straining prior to failure.

The high strength of the nc 316L stainless steel is attributed to the grain size effect in terms of Hall–Petch (H–P) relation. Fig. 3 shows a H–P plot using measured  $\sigma_y$  of 316L pure-austenite stainless steel reported in the literature (as listed in Table 1). Extrapolating the H–P line down to the nanometer scale, one may find that present results (both the average  $\sigma_y$ , data from 4 tensile tests and the average hardness value from thirty indent data) of the nc sample fit the H–P line very well. It implies strengthening of the present 316L originates merely from the grain refinement effect in the nanometer scale, in which lattice dislocation motions are blocked by numerous amount of grain boundaries. This observation

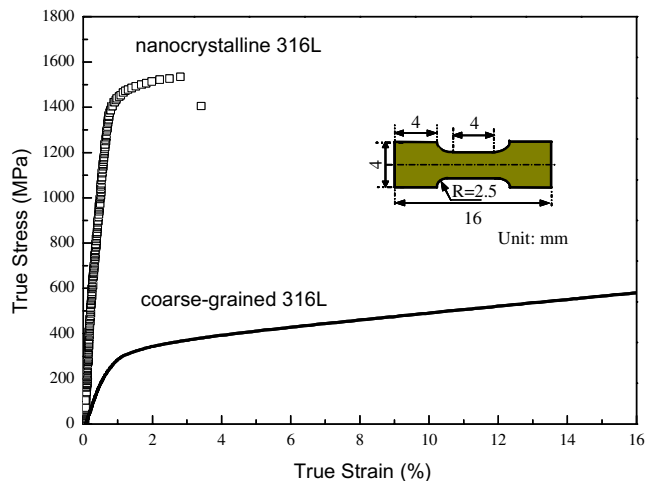


Fig. 2. Tensile true stress-strain curves for the nc and the CG 316L samples. Insert shows the geometry of the tensile specimen.

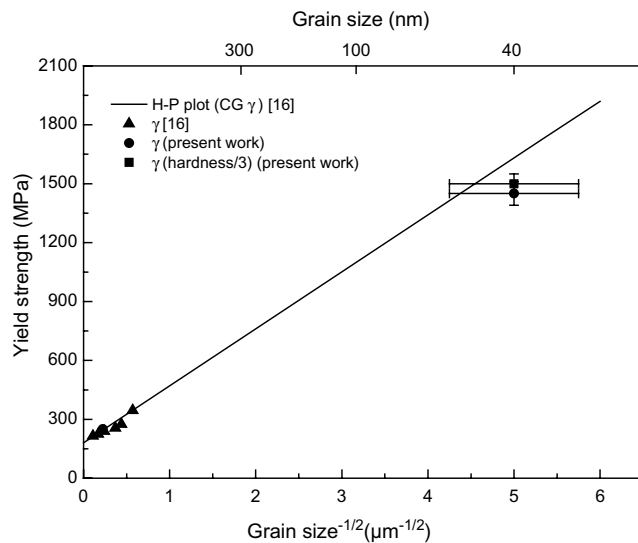


Fig. 3. Plot of the tensile yield strength and microhardness (divided by 3) as a function of the inverse square root of mean grain size using measurement results reported in the literature and in this work for 316L.

is consistent with previous experimental results that hardness values of nc iron samples with mean grain sizes of 6–60 nm were still in general agreement with the H–P relationship [12]. The depressed plasticity in the nc 316L sample can be attributed to reduced dislocation activities confined within tiny grains.

In general, the SMAT sample could be strengthened by grain boundaries, internal stress and solute elements. Although the residual compressive stresses could be induced by SMAT processing in the nc samples, the macroscopic residual stresses were relaxed after the thin layer of nanostructure was taken off because the gradi-

ent of the macrostress is quite small between the top and the bottom of thin specimens [13]. Therefore, the 316L thin samples can be regarded as the macrostress free specimens, and the contribution of the residual stresses to the observed high strength is believed to be very small [14].

The SMAT technique is a unique technique, which produces nanostructured samples via severe plastic deformation. It does not introduce contaminations into the nanostructured sample [7,8]. X-ray diffraction and SAED analysis of the SMAT 316L samples showed that there is no martensite phase or other impurities in the SMAT samples. So the strengthening effect of martensite in the present high strength 316L stainless steel can be ruled out. The impurity effect on strengthening is also negligible.

Fracture surface morphologies after tensile test for nc 316L sample are shown in Fig. 4. Two kinds of typical fracture patterns are observed in the nc sample, marked as A and B, due to the variation of grain sizes along the sample thickness. It seems the A patterns (related to the top surface with nanometer-sized grains) is dominated by shear bands, appearing in groups and tending to be parallel to one another with a width of 0.4  $\mu\text{m}$ . However, the B pattern (with a larger grain size) presents a rough and irregular surface structure. The fracture morphologies suggest that nc 316L sample plastically deformed in the regions with coarse grains (submicro-sized, of which  $\sigma_y$  is lower than that of the nanosized layer) until it was finally torn apart when the fracture strength of the material was exceeded. In addition, a few dimples have been observed in the fracture surface between region A and B (as shown in Fig. 4(b)), which is consistent with a little plastic strain in the nc sample.

Mechanical properties for 316L with different processing conditions are listed in Table 1. A martensite transformation is a prevailing phenomenon in the plastic deformed 316L austenitic stainless steel. As a reinforcing phase, martensite can effectively enhance the strength of 316L [15]. When a 316L plate was cold rolled at 77 K for a reduction of 80%, the metastable austenite was entirely transformed to martensite, with which a yield strength exceeding 1600 MPa was obtained, which is the highest yield strength value so far for 316L stainless steel [4]. However, for the 316L without a martensite phase, the present nc 316L sample processed by means of SMAT shows the highest yield strength of 1450 MPa.

The ultrahigh strength of nc 316L would make it useful in applications in micro-electromechanical systems (MEMS) based on 316L. In addition, with this ultrahigh strength nc 316L, one may expect that  $\sigma_y$  of a 1 mm thick 316L plate can be doubled if both sides of the plate are processed by means of SMAT to generate a nc layer of  $\sim 20 \mu\text{m}$  thick on surfaces. Such an experiment was performed and a  $\sigma_y$  of about 550 MPa was obtained for the 1 mm thick 316L sheet (280 MPa for the original



Table 1  
Mechanical properties of 316L at room temperature

Structure	Processing conditions	Average grain size	UTS (MPa)	Yield stress (MPa)	Elongation (%)	Hardness (GPa)	References
$\gamma$	SMAT	40 nm (TEM)	1550 $\pm$ 80	1450 $\pm$ 60	3.4 $\pm$ 0.4	4.5	Present work
	90% CR at 298 K	—	1380	1290	3.2	4.5	[4]
	50% HR at 1273 K + 80% CR at 298 K	—	1450	1290	6	—	[4]
	90% CR at 293 K + annealed	3.1 $\mu$ m	—	360	—	—	[16]
	90% CR at 293 K + annealed	5.1 $\mu$ m	—	290	—	—	[16]
	90% CR at 293 K + annealed	7.3 $\mu$ m	—	260	—	—	[16]
	90% CR at 293 K + annealed	16.8 $\mu$ m	—	235	—	—	[16]
	90% CR at 293 K + annealed	33.1 $\mu$ m	—	220	—	—	[16]
	90% CR at 293 K + annealed	86.7 $\mu$ m	—	210	—	—	[16]
$\gamma + \alpha$	Coarse-grained	20 $\mu$ m	630	250	55	2.0	Present work
	100% $\alpha$ 80% CR at 77 K	—	1920	1670	2.9	5.6	[4]
	40% $\alpha$ 80% CR at 77 K + 873 K/10 min	100 nm (TEM)	1610	1280	3.2	5.4	[4]
	10% $\alpha$ 80% CR at 77 K + 973 K/10 min	300 nm (TEM)	1400	1190	5	4.7	[4]
	— HPT	65 nm (TEM)	1340	—	—	—	[5]
	50% $\alpha$ 15% CR at 77 K	—	1050	680	12	—	[14]
	100% $\alpha$ MM + 1173 K/3.6 ks VHP	250 nm (TEM)	—	—	—	6.2	[3]

CR: cold rolling; HR: hot rolling; HPT: high pressure torsion; MM: mechanical milling; VHP: vacuum hot pressing; UTS: ultimate tensile stress; elongation: elongation-to-failure in tensile tests.

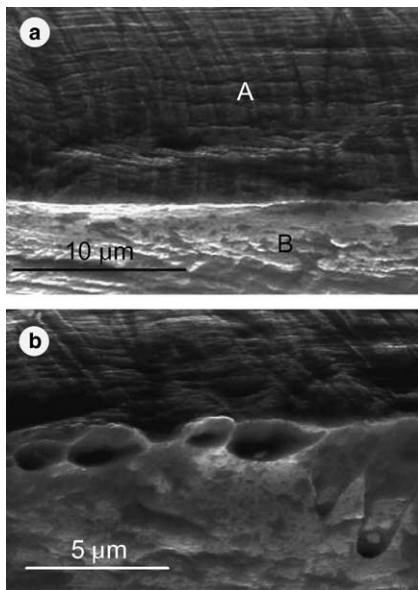


Fig. 4. Typical SEM fractographs showing fracture surfaces of the nc 316L tensile sample.

sheet) [13]. This result indicated a novel approach to significantly strengthen stainless steel sheets while keeping its austenitic structure by producing nc surface layers using SMAT.

#### 4. Summary

A nanocrystalline 316L austenitic stainless steel sample was prepared by means of the SMAT technique. Uniaxial tensile tests at room temperature showed that nc 316L sample exhibits a yield strength as high as

1450 MPa, which is about six times higher than that of a CG sample. This ultrahigh strength of the nc sample, which still follows the H–P relation extrapolated from CG structures, is attributed to the effective blockage of lattice dislocation motions by nanometer-sized grains. The ultrahigh strength nc stainless steel may find potential applications in MEMS and in strengthening stainless steel sheets by using SMAT processing.

#### Acknowledgements

This work was supported by NSF of China (Grants No. 50021101 and 50201017), Ministry of Science and Technology of China (G1999064505), the NEDO International Joint Research Grant Program (01MB5), and the French Ministry of Research (Grant 2001882, CPER EN2040).

#### References

- [1] Pelletier H, Muller D, Mille P, Cornet A, Grob JJ. Surf Coat Technol 2002;151:377.
- [2] Rawers J, Crogon F, Krabbe R, Duttlinger N. Powder Metall 1996;39:125.
- [3] Fujiwara H, Ameyama K. Mater Sci Forum 1999;304–306:47.
- [4] Uçok I, Ando T, Grant NJ. Mater Sci Eng A 1991;133:284.
- [5] Pakielka Z, Sus-Ryszkowska M, Druzycka-Wieniec A, Kurzydowski KJ. Seventh Int Conf on Nanostructured Materials, Germany, 20–24 June 2004.
- [6] Harvey PD. Engineering properties of steel. Metals Park, Ohio: American Society for Metals; 1982. p. 243.
- [7] Lu K, Lu J. J Mater Sci Tech 1999;15:193.
- [8] Lu K, Lu J. Mater Sci Eng A 2004;375–377:38.
- [9] Tong WP, Tao NR, Wang ZB, Lu J, Lu K. Science 2003;299:686.

- [10] Tao NR, Wang ZB, Tong WP, Sui ML, Lu J, Lu K. *Acta Mater* 2002;50:4603.
- [11] Liu G, Lu J, Lu K. *Mater Sci Eng A* 2000;286:91.
- [12] Jang JSC, Koch CC. *Scripta Metall Mater* 1990;24:1599.
- [13] Lu J, Lu K. In: Milne I, Ritchie RO, Karihaloo B, editors. *Comprehensive structural integrity*. Oxford: Elsevier; 2003. p. 495.
- [14] Wang YM, Wang K, Pan D, Lu K, Hemker KJ, Ma E. *Scripta Mater* 2003;48:1581.
- [15] Spencer K, Embury JD, Conlon KT, Veron M, Brechet Y. *Mater Sci Eng A* 2004;387–389:873.
- [16] Kashyap BP, Tangri K. *Acta Metall Mater* 1995;43:3971.